Junction-Aware Extraction and Regularization of Urban Road Networks in High-Resolution SAR Images

Matteo Negri, Paolo Gamba, *Senior Member, IEEE,* Gianni Lisini, *Member, IEEE,* and Florence Tupin, *Member, IEEE*

***Abstract*—A general processing framework for urban road network extraction in high-resolution synthetic aperture radar images is proposed. It is based on novel multiscale detection of street candidates, followed by optimization using a Markov random field description of the road network. The latter step, in the path of recent technical literature, is enriched by the inclusion of *a priori* knowledge about road junctions and the automatic choice of most of the involved parameters. Advantages over existing and previous extraction and optimization procedures are proved by comparison using data from different sensors and locations.**

***Index Terms*—High-resolution synthetic aperture radar (SAR), Markov random fields (MRFs), road network, urban remote sensing.**

I. Introduction

ROAD network reconstruction in remote sensing imagery has been widely analyzed, both considering high-resolution optical [1] and coarse-resolution synthetic aperture radar (SAR) data [2]. Only recently and in light of the advent of new satellites carrying high-resolution SAR sensors, works about road network extraction from high-resolution SAR data have started to appear [3], [4]. Indeed, SAR data coming from the new TerraSAR-X and RADARSAT-2 sensors will provide ground spatial resolutions adequate for road extraction even in urban areas.

It is generally acknowledged that a good methodology for road network extraction needs to accomplish two separate tasks, namely: 1) an efficient way to detect lines and curves and 2) a good strategy to recover the network and suppress false positives. As for the first step, there are many works addressing edge detection in SAR imagery, even high-resolution ones, that may be used for road candidate extraction. For high-resolution data, adaptive directional filtering [5], statistical analysis [6], and coherence filtering [7] have been developed.

Far fewer works have been proposed on network topology reconstruction after road extraction in SAR imagery. Relevant literature lists Markov random fields (MRFs) [8], [9] or genetic algorithms [10], but research work is still ongoing. One may of course apply optimization schemes originally developed for optical images [11]–[13], but even these methods do not comply with any urban situation. Moreover, they may imply road extraction efficiency not met in urban area SAR imagery because of well-known shadowing and layover effects [14]. For instance, Price [12] looks for orthogonal crossroad patterns and propagates the network along the directions of the junction branches, and this may be a problem in urban areas outside North America. Dead ends and more complex urban networks are not fully extracted with the algorithm in [11], and a spatial resolution well beyond current SAR systems would allow using the approach in [13].

It is thus our feeling that, as for road network reconstruction in urban areas by means of high-resolution SAR imagery, there is room for research work in both road extraction and road network optimization.

Road extraction in high-resolution SAR data may be improved because recovering roads from edges is only a partially efficient approach. In fact, with meter or submeter spatial resolution, roads in SAR data may be more precisely modeled as dark elongated areas surrounded by bright edges, which are due to double-bounce reflections by surrounding buildings or uniform backscattering by the vegetation. A way to exploit all the information may be to jointly use the extracted edges and a classification map of the same area [15], but this requires a parallel and usually supervised classification step. A different approach, which is suggested in this research work, is to perform a feature fusion step using detectors suited to both edge and dark elongated area detection.

On the subject of network reconstruction, it has been recently proved [14] that, in normal illumination conditions and with a European urban structure, nearly half of the road network is invisible to SAR sensors due to shadowing and layover effects. One suggested way to improve extraction is to fuse networks coming from different views of the same area [16], taking account also of junctions. However, this is only partially an advantage for spaceborne sensors because of the fixed orbits. Thus, it is still worth trying and exploiting, as much as possible, the information available by one single scene. The idea underlying this paper is that *a priori* knowledge about road junctions may help to infer the presence or absence of roads even if they are not actually visible in the imagery. Thus, the proposed procedure relies on candidate junction identification as a further means to guide the network topology optimization process. Junctions have already been exploited in [12] and [17]

Manuscript received November 25, 2005; revised April 19, 2006.

M. Negri was with the Dipartimento di Elettronica, Universitá di Pavia, I-2700 Pavia, Italy. He is now with the Digitec Lecco srl, 36075 Montecchio Maggiore (VI), Italy.

P. Gamba and G. Lisini are with the Dipartimento di Elettronica, Universitá di Pavia, I-27100 Pavia, Italy (e-mail: paolo.gamba@unipv.it).

F. Tupin is with the Traitement du Signal et des Images École Nationale Supérieure des Télécommunications, 75634 Paris, France.

Digital Object Identifier 10.1109/TGRS.2006.877289

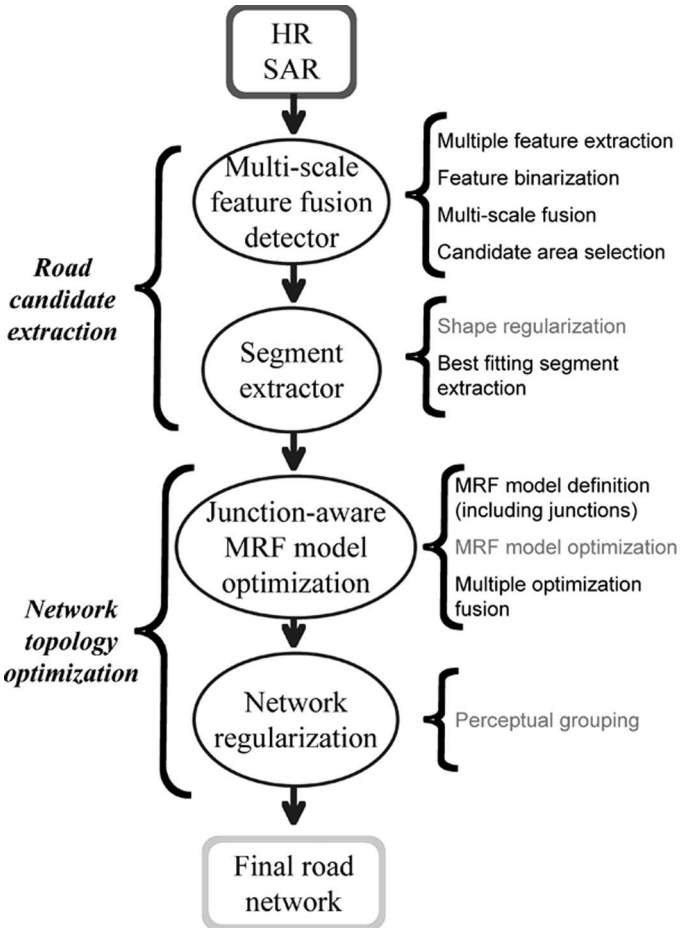

Fig. 1. Workflow of the proposed algorithm. The processing steps in light gray are not novel parts of this work.

for network analysis, and algorithms for junction extraction and refinement in optical images are also available [18], [19]. The novelty of this paper relies in the introduction of junction hints in the network optimization process, which is described by means of a modified MRF model. This is done by first detecting candidate T- and L-shaped junctions and then forcing roads to pass through them.

The conceptual workflow of the proposed procedure is shown in Fig. 1 and, as stated before, consists of two steps. The first is road candidate extraction, which is further specified into a multiscale feature fusion detector and a segment extractor, as discussed in Section II. The second is network topology optimization (Section III), which is again further specified into a junction-aware MRF model optimization and a final network regularization step based on perceptual grouping concepts.

The procedure is tested in Section IV, where results on different high-resolution SAR data are presented and the parameters involved in the procedure are discussed. Section V closes this paper with some conclusions and ideas for future work.

II. Road Candidate Extraction

Aside from providing the conceptual framework of the overall procedure, Fig. 1 also shows in detail the processing steps that implement the multiscale feature fusion detector (multiple-feature extraction, feature binarization, multiscale fusion, and candidate area selection) and the segment extractor (shape regularization and best fitting segment extraction). Steps not specifically developed in this paper are listed in light gray.

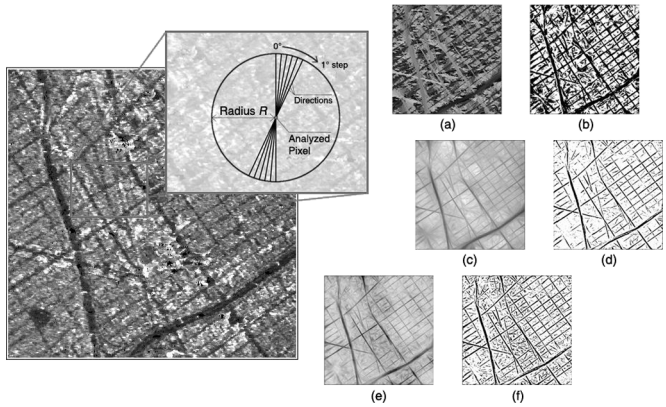

Fig. 2. Feature extracted from a sample SAR image. (a) θ_0. (c) r_0. (e) c_0. (b), (d), and (f) Corresponding binarized values.

A. Multiscale Feature Fusion Detector

Road candidate extraction in high-resolution imagery usually starts with road area detection, which of course may be obtained in optical images by looking for the spectral response of road materials. However, road class recognition in high-resolution SAR data would imply complex segmentation algorithms based on data statistics. In this paper, it is preferred to prove that multiple detectors may be enough to obtain good results. Moreover, it should be stressed that road detection does not imply immediately that attention is paid to road junctions. Instead, as shown later in the text, in the proposed strategy, junctions play a crucial role, and junction information must be preserved. Therefore, in this paper, a new extraction method based on multiple-feature detection, designed to be as automatic as possible, and aimed at optimal junction preservation is proposed. The algorithm exploits spatial relationships between a pixel and its neighbors, looking for straight features in the image and combining multiple detectors to improve road candidate detection. This strategy follows the achievements of [20]–[22], where multiple detectors were combined into a consistent framework for SAR imagery, but with a new and more efficient algorithm.

In high-resolution SAR images, as discussed previously, roads are no more a subset of image edges. Instead, they usually appear as dark elongated areas with bright lateral edges. Therefore, one may detect roads by looking for pairs of parallel edges or searching for dark homogeneous areas. Both of these methods, however, are subject to false positives (e.g., other artificial structures and low-reflectance areas, respectively). A more precise approach may be one using a combination of these ideas. This is the aim of the following algorithm, which furthermore integrates road features into a multiscale-feature fusion framework.

1) Multiple-Feature Extraction: In order to search for road pixels, the first step in this procedure is the computation of a few spatial features in a circular window around the current pixel $p(i, j)$ (Fig. 2). Of course, each of these features will be a function of the window radius R.

Given the total radiance $r(i,j,R,\theta)$ along the direction identified by angle θ, which can be expressed as

$$r(i,j,R,\theta)=\sum_{k=-R/2}^{R/2} p\left([i+k\cos(\theta)],[j+k\sin(\theta)]\right) \quad (1)$$

the direction with lower total radiance

$$\theta_0(i,j,R)=\arg\min_{\theta} r(i,j,R,\theta),\ \theta\in\{0^\circ,1^\circ,2^\circ,\ldots,178^\circ,179^\circ\} \quad (2)$$

and the corresponding mean radiance value $r_0(i,j,R)=r(i,j,R,\theta_0)$ are computed.

These features highlight dark elongated areas in the pixel neighborhood. If they are good candidates for road areas, a high contrast is also expected between r_0 and the average total radiance along all 180 directions. A check is provided by computing

$$c_0(i,j,R)=\left\|\frac{\sum_\theta r(i,j,R,\theta)}{180}-r_0(i,j,R)\right\|. \quad (3)$$

It is clear that θ_0, r_0, and c_0 show different information. The first value [Fig. 2(a)] highlights the most likely direction for dark elongated areas in the image, whereas the second and third ones [Fig. 2(c) and (d)], respectively, quantify how dark and contrasted these areas are. All of that apply only for a given spatial scale defined by R.

In summary, the proposed features capture different but consistent characteristics of roads, which locally may always be considered as modeled by dark straight segments. Therefore, they lead to almost the same findings but possibly (Fig. 2) with different false recognitions. This point may be used to combine them and provide better extraction results.

2) Feature Binarization: The following step in road candidate extraction is a semiautomatic feature binarization. The aim of this step is to select significant values for θ_0, r_0, and c_0 and focus the extraction algorithm only on interesting areas.

Roughly speaking, binarization would require the selection of a threshold. This threshold may set globally, but a much more efficient algorithm is to set it locally, looking for the neighborhood of the position under test. By this choice, only positions with feature values significantly similar to (or different from) their neighborhood are labeled and retained.

In this paper, binarization is thus obtained by comparison between the pixel feature value and its neighborhood. More specifically, for $\theta_0(i,j,R)$, a position is retained if its absolute difference from its local average value $\overline{\theta_0(i,j,R)}$ is smaller than an experimental value T_θ, which can be expressed as

$$\theta_0^{(b)}(i,j,R)=\begin{cases}0, & \text{if } \left|\theta_0(i,j,R)-\overline{\theta_0(i,j,R)}\le T_\theta\right|\\ 1, & \text{if } \left|\theta_0(i,j,R)-\overline{\theta_0(i,j,R)}> T_\theta\right|\end{cases}. \quad (4)$$

TABLE I
PARAMETERS FOR FEATURE BINARIZATION

feature	threshold	window width
θ_0	$T_\theta = 12^\circ$-R/5	17 pixels
r_0	$T_r = 0.92$	9 pixels
c_0	$T_c = 0.92$	9 pixels

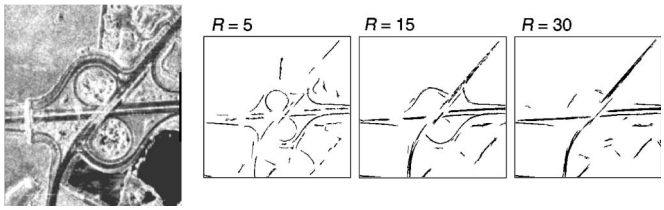

Fig. 3. Multiscale feature maps for a highway roundabout, showing that different scales depict different details of the original data (R in pixels).

For r_0 and c_0, the tested quantity is instead the ratio between the current value and the local average, again using experimental thresholds, i.e.,

$$r_0^{(b)}(i,j,R)=\begin{cases}0, & \text{if } r_0(i,j,R)/\overline{r_0(i,j,R)}\ge T_r\\ 1, & \text{if } r_0(i,j,R)/\overline{r_0(i,j,R)}< T_r\end{cases} \quad (5)$$

$$c_0^{(b)}(i,j,R)=\begin{cases}0, & \text{if } c_0(i,j,R)/\overline{c_0(i,j,R)}\ge T_c\\ 1, & \text{if } c_0(i,j,R)/\overline{c_0(i,j,R)}< T_c\end{cases}. \quad (6)$$

In summary, the black (significant) areas in Fig. 2(b), (d), and (f) correspond to areas where each feature is "sufficiently" homogeneous at a given scale. Because of the different nature of the information highlighted by each feature, different window widths are considered for local average computation. All parameters are listed (with implemented values) in Table I.

3) Multiscale Fusion: In order to exploit multiple scales, the previous steps are performed with values of $R\in\mathbf{R}=\{R_1,R_2,\ldots,R_N\}$. In the end, a binary feature map $f(i,j)$ is computed as a logical AND across binarized features at all scales and is given by

$$f(i,j)=\wedge_{\mathbf{R}}\left(\theta_0^b(i,j,R)\wedge r_0^b(i,j,R)\wedge c_0^b(i,j,R)\right). \quad (7)$$

The final feature map is therefore the result of a multiscale feature fusion, which allows detecting different features of candidate road regions at multiple scales and using multiple detectors. Fig. 3, where the procedure is applied to a highway roundabout, depicts why more scales are required, with the smaller R prizing shorter and thinner road candidates and the larger R prizing longer and wider roads.

4) Area Selection: The last step of the processing chain for multiscale feature fusion detection is the selection of candidate regions in the binary multiscale feature map. To this aim, a spatial and a spectral criterion are employed.

The spatial check discards small-area regions that, according to the ground spatial resolution of the sensor, could not be elements of the road network. To this aim, only regions with an area greater than 16 pixels are considered.

The second check is instead based on spectral information and discarded areas whose average radiance value is much

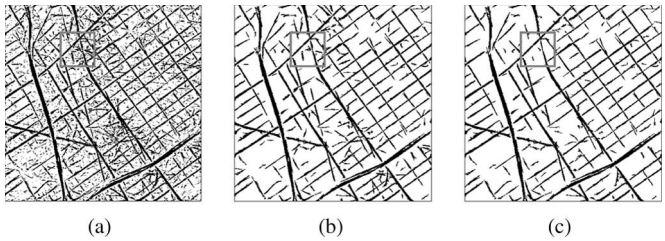

Fig. 4. Feature map for the original SAR image in Fig. 2. (a) After the multiscale AND. (b) After the geometrical check. (c) After the spectral check.

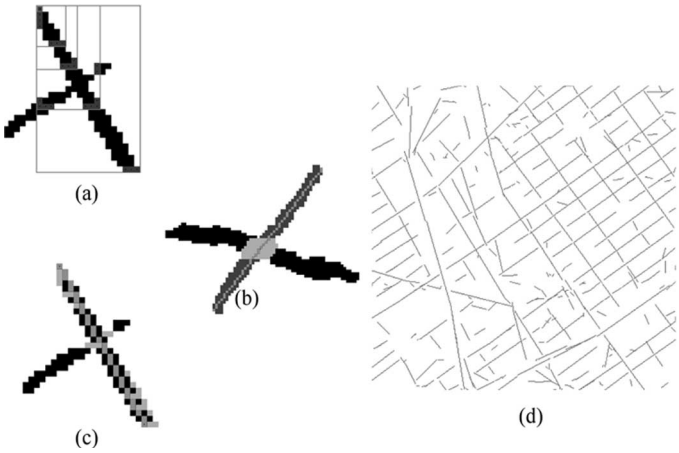

Fig. 5. Straight segment extraction. (a) Tracking procedure. (b) Junction detection. (c) Segment extraction. (d) Final vector map from Fig. 4(c).

higher from the mean value of the overall data set r_m. To this aim, the average area value is computed, and it should be smaller than $1 + 1/3 \times r_m$.

The multiscale feature map for the image in Fig. 2 is shown in Fig. 4(a). In Fig. 4(b) and (c), road candidates not passing the first and the second check are deleted, respectively.

B. Segment Extraction

After carefully determining the candidate regions for the road network, we need to vectorize the result, translating selected paths into segment chains. This is done in two steps. The first is aimed at shape regularization for each candidate region, which may be composed of multiple connected road segments (Fig. 5). The second step is aimed at the extraction of the segment chain that best fits the region shape, possibly including multiple branches.

1) Shape Regularization: This step is performed very simply by a morphological closing with a 3×3 square element, which is aimed at reducing small gaps and irregularities along the edges of the selected candidate road regions.

2) Best Fitting Segment Extraction: Far more complex is the following step because of the unknown number of branches in each candidate region. Instead of working through a skeletonization similar to that in [23] and then applying a routine approximating the skeleton with a linear segment chain [24], in this paper, the best fitting segments for the region skeleton are directly extracted using an incremental tracking approach.

Starting from a random pixel in a candidate road region, a rectangular window is opened and iteratively widened in the vertical and horizontal direction until no more road pixels may be added. Fig. 5(a) shows an example where an edge pixel is used as the initial seed. Once the final window is settled, the best fitting segment for the area inside this window is extracted. The detector described in Section II-A assures that each pixel in a candidate region belongs to an elongated-road candidate area. Thus, it is reasonable to approximate the portion of the region in the selected window by a single straight segment.

To select this segment, all those connecting road pixels at the top of the window to those at the bottom are tested. For each segment, an index is computed, which is equal to the number of pixels with no match on the other side of the segment either vertically or horizontally. As an example, in Fig. 5(c), horizontally unmatched pixels are drawn in green. The segment with the lowest index value is selected.

However, the procedure needs to maintain the information about junctions along the retrieved segment to preserve the extraction of intersecting roads. To this aim, the average vertical and horizontal widths of the road area along the extracted segment path are computed. Parts of the region with a local width higher than 120% of the average value are preserved as "ancillary" regions for the extraction of intersecting segments. Note, however, that these regions cannot provide a segment by themselves but only in conjunction with other regions to prevent extraction of duplicated linear features.

The aim of the best fitting extraction routine is therefore twofold.

1) It works to extract fewer and longer road segments, even for roads with multiple junctions along their path. This allows the reduction of the computational load of the following network topology optimization step, which increases exponentially with the number of candidate segments.
2) The routine precisely reconstructs the intersecting roads in a junction [e.g., Fig. 5(b)].

Fig. 5(d) shows the results of the final vectorization starting from Fig. 4(c). Please note that the overall number of road candidates with the proposed method is reduced by 60% in the proposed example (exactly, from 901 to 367) with respect to those extracted using the procedure in [24].

III. Network Topology Optimization

The second part of this paper explains the proposed road network optimization scheme based on global as well as local methods. Looking again at Fig. 1, the first step is a global optimization based on a junction-aware MRF model of the network, which is further specified into an MRF model definition, MRF model optimization, and multiple optimization fusion. A locally based final network regularization is then carried out by means of perceptual grouping rules. Please note that this part exploits processing techniques coming from earlier works, which are highlighted in Fig. 1 by using a lighter gray tone. Pointers to relevant literature will be proposed for these steps, whereas a more detailed presentation will be provided in the following paragraphs for the novel parts of the procedure.

A. Junction-Aware MRF Model Optimization

Road network optimization by means of an MRF model has been initially proposed in [8] and refined in [16]. This model already introduces contextual knowledge about the topological characteristics of any road network, such as a certain degree of regularity, the preference for low curvature, and so on, in the optimization process. This paper proposes two additions to the original model, together with a slight change in the selection of the main parameters of the MRF optimization chain.

1) MRF Model Definition: Let us first briefly recall, following [8], the notation for an MRF-based description of the road network. The set of detected road candidates is S_d, and the set of possible connections is S'_d. A "connection" is a candidate junction in the retrieved road network, as explained in the following. In [8], the threshold for selecting possible connections is based on the maximum length of the detected ones, which is called $D_{\max}$. However, this is a rather unusual assumption in urban areas especially after a good road candidate extraction process. Instead, we expect that missing connections are shorter than extracted candidate roads in most cases.

Thus, this paper proposes to choose $D_{\max}$ in a different way. In particular, first, the average value of the shortest five connections between the ith road candidate and any other extracted segment, which is called H_i, is computed. Then, a global average of H_i over S_d is computed, leading to

$$D_{\max} = \overline{H_i}. \tag{8}$$

By this choice, the maximum length of a possible connection is computed by a global average of a locally defined mean connection length. Only five gaps are considered at the local state because five is the usual maximum number of branches in a junction.

Together with this slightly different definition for $D_{\max}$, in this paper, it is proposed to add a second selection parameter to define S'_d, which is aimed at reducing not only the length range but also the orientation range of undetected elements of the road network. The second parameter, which is called $\theta_{\max}$, is computed according to

$$\theta_{\max} = \sqrt{\overline{(\theta_i - \theta_j)^2}} \tag{9}$$

where θ_i is the orientation of segment $i \in S_d$.

Now, let us denote by M_i^k, $k = 1, 2$ the endpoints of segment i. A connection between segment i and segment j, which are both $\in S_d$, is labeled as possible and added to S'_d if [Fig. 6(a)]

1) it links two endpoints of segments, i.e., $\in \{M_i^k M_j^l,\ k = 1, 2;\ l = 1, 2\}$;
2) the endpoints are close enough (i.e., the distance between them is less than $D_{\max}$);
3) the alignment of the two segments is acceptable (i.e., $|\theta_i - \theta_j| \leq \theta_{\max}$).

Note that the meaning of (9) is that the directional variability of possible connections is limited by the orientations of the elements in S_d. $\theta_{\max}$ is small if segments in S_d tend to gather around one or two main directions (which is the case for an ordered urban road network). If a less ordered situation is considered, a wider range of directions is also allowed in S'_d.

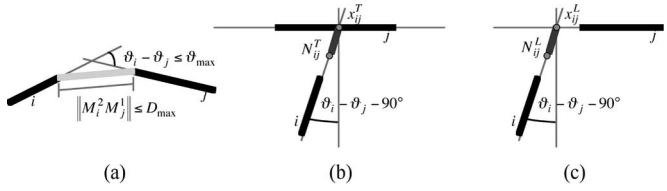

Fig. 6. Parameters of the MRF-based road network optimization. (a) Normal situation. (b) Candidate T-shaped junction. (c) Candidate L-shaped junction.

Finally, in addition to these very simple parameter changes, this paper proposes to introduce explicitly in the MRF model the information about missing (but probable) junctions. In particular, the idea is to recognize where T- and L-shaped junctions may occur and build a junction-aware MRF model. The approach is somehow similar to that in [17], where "junction hypotheses" are proposed and evaluated, but with a different candidate junction definition and evaluation methodology.

The modified MRF model requires that two new segment sets S_d^T and S_d^L are added to the original S_d set. More precisely, S_d^T is built by recognizing candidate T-shaped junctions as follows: A candidate T-shaped junction is defined as a set of two segments i and j with an absolute difference in orientation $|\theta_i - \theta_j|$ in a range of $\theta_{\max}$ around 90°. Furthermore, the intersection point x_{ij}^T between the lines identified by the two segments lays on segment i or segment j and is within a range of $D_{\max}$ from the nearest endpoint of the other segment [Fig. 6(b)].

Let N_{ij} denote the middle point of the connection from x_{ij}^T to the nearest endpoint of the other segment. Then, S_d^T is made by a "trap segment" for each candidate junction, which spans half of the missing connection back from the intersection point to the incident segment

$$S_d^T = \left\{x_{ij}^T N_{ij}^T,\ i \in S_d;\ j \in S_d;\ x_{ij}^T \in (i \cup j);\ |\theta_i - \theta_j - 90°| \leq \theta_{\max}\right\}. \tag{10}$$

Similarly, candidate L-shaped junctions are defined as a set of two segments satisfying the same orientation constraints than for T-shaped junctions. However, now, the intersection point x_{ij}^L is external to both of them but within a $D_{\max}$ distance from the closest endpoints. S_d^L is thus composed of segments forced to existence and covering half the missing path in the direction of the segment that is farther from x_{ij}^L [Fig. 6(c)]. Denoting with N_{ij}^L the middle point of this missing path, we have

$$S_d^L = \left\{x_{ij}^L N_{ij}^L,\ i \in S_d;\ j \in S_d;\ x_{ij}^L \notin (i \cup j);\ |\theta_i - \theta_j - 90°| \leq \theta_{\max}\right\}. \tag{11}$$

Note that by adding S_d^T and S_d^L to the original set S_d, S'_d is also forced to include all the missing connections to the newly introduced trap segments because these connections are by definition inside the proposed length and directional ranges. This is especially important for T-shaped candidate junctions. In fact, they were impossible recognize in [8], where only endpoint connections were considered. The present modified

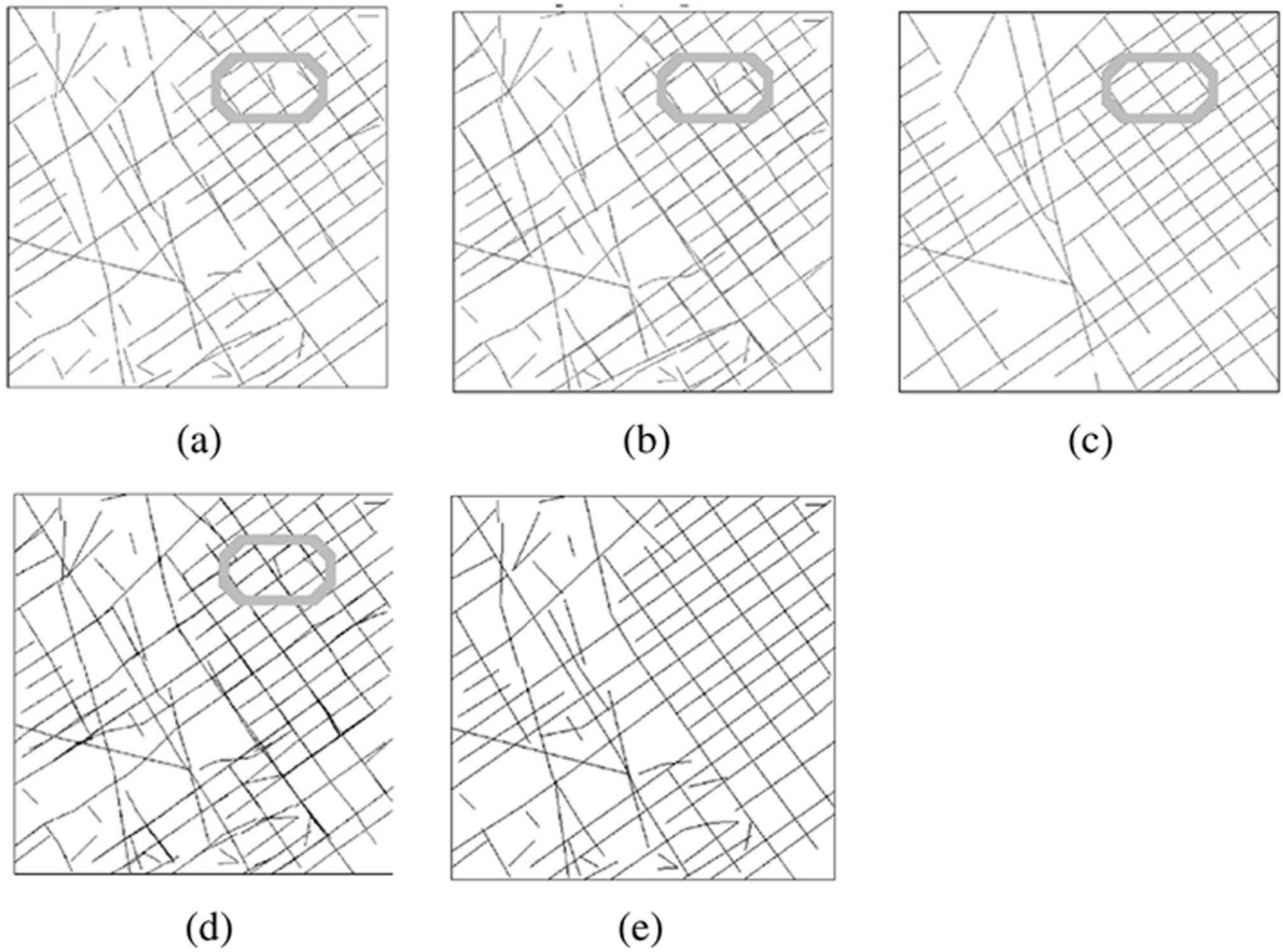

Fig. 7. Comparison of the MRF optimization results. (a) Without *a priori* knowledge about junctions. (b) With knowledge about L- and T-shaped junctions. (c) Ground truth. (d) Using the multiple optimization approach. (e) After the final network regularization step.

model includes instead the *a priori* knowledge that urban road networks prize connections through junctions, even if this forces higher local road curvatures.

It is worth adding here a comment about the comparison between the approach presented in this paper and the methodology discussed in [16], where a modified MRF model with junctions is also considered. The main difference is in the extraction approach, which provides here longer and more precise roads and, therefore, offers a more refined input around junctions and even outside junction areas to MRF optimization. The second difference is, however, in the junction definition. For the sake of simplicity, let us focus on a T-shaped junction. In [16], it is defined as a set of three segments (either detected or undetected) having a common endpoint. In this paper, in addition to this definition, we add the possibility to have a T-shaped junction when there is a point inside an already detected segment where another detected segment may join it. In other words, a T-shaped junction is still a set of three segments (two detected and one undetected), but they have no common endpoint. This new definition adds flexibility to the approach and improves its ability to detect potential junctions that may split segments.

2) MRF Model Optimization: Following the modified MRF model discussed in the previous sections, optimization of the complete set $S = S_d \cup S_d^T \cup S_d^L \cup S_d'$ is carried out by associating potentials to each element [8]. This may be reduced to the minimization of the energy functional

$$U = \sum_{i \in S} V_i + \sum_{c \in C} V_c \tag{12}$$

where, with a slightly simplified notation than in [8], V_i is the potential of the ith segment, which is linked to its conditional probability, and C is the set of considered spatial aggregations of one or more segments in MRF notation called "cliques."

The minimum of the global energy function U is reached using the pretty much standard iterated conditional mode (ICM) approach [25]. In our implementation, unlike that of [8], results are stable and reach stability very quickly, e.g., 2 s on a standard personal computer and a total set of 300 segments. Stability has been observed by comparison with more complex algorithms for minimum search and is due to the excellently conditioned segment set, which is provided as input to the MRF.

3) Multiple Optimization Fusion: As one would expect, the junction-aware MRF model optimization, as proposed previously, is able to provide good results. In fact, it improves the results with respect to the original MRF approach in [8], works in a semiautomatic way and, which is the most important fact

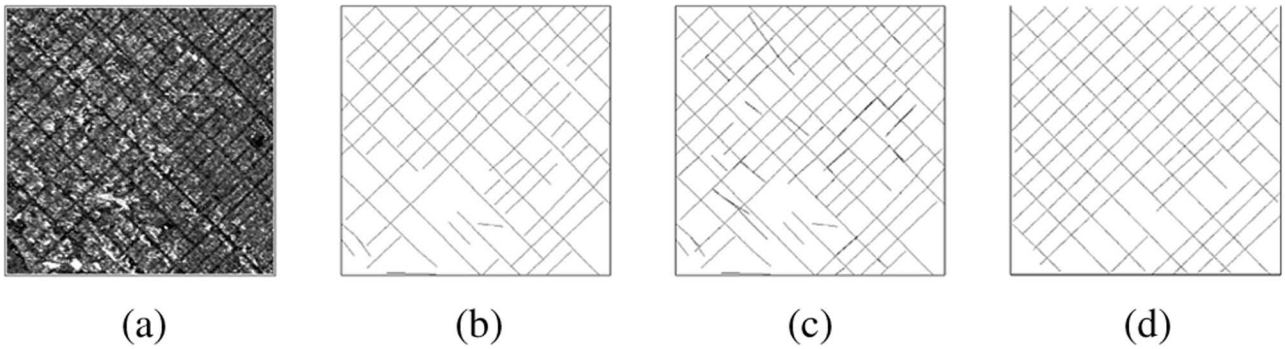

Fig. 8. Second test area in the AIRSAR data set. (a) Original SAR image. (b) Road network obtained by the present procedure without considering junctions. (c) Road network considering junctions. (d) Raster representation of the corresponding ground truth.

from our point of view, allows considering urban areas where junctions are crucial. For example, results for the SAR image in Fig. 2 may be compared in Fig. 7(a) and (b), where results without and with L- and T-junction knowledge are shown, respectively, and both should be compared with the ground truth in Fig. 7(c). More real junctions are now in the final network, and missing roads are partially recovered, as shown in the highlighted area of the image. However, Fig. 7(b) still has some problems, for instance, in the very same area.

As a matter of fact, a long and detailed analysis of all the options proved that best results may be achieved using "multiple optimization." More precisely, first, the original MRF optimization without any knowledge about junctions is run. Then, two more optimizations are computed, adding only T-shaped or L-shaped junctions, respectively. The three results are combined in the simplest possible way, i.e., by a logical AND operation to take advantage of all of them. For the same image, this procedure leads to Fig. 7(d). Better recognition of roads is now achieved than in the previous situation.

The experimental reason for this behavior is the relatively large number of candidate T- and L-shaped junctions in a usual urban network. If they are not considered, the result is the poorest one. However, if all of them are simultaneously taken into account, the optimization problem becomes too complex and the ICM approach does not work at its best. More investigation is indeed worth on this topic.

B. Network Regularization

The drawback of the multiple optimization fusion step is the greater complexity of the final fused network, which is usually with many duplications. Therefore, a final network regularization algorithm is implemented based on perceptual grouping concepts. It is aimed not only at reducing overlapping segments but also at grouping still unconnected road elements according to some rules on their local mutual positions. These rules have been introduced in [5] and are one of the topics of a recently accepted publication [26]. Thus, they are only briefly outlined here.

The perceptual grouping rules used in this step are quite basic and are based on proximity and collinearity concepts. The rule set is very similar to that in [27] but with a few changes to take into account junctions and other peculiarities of road networks in urban areas. Basically, four steps are performed in a sequence.

1) A proximity check is performed, and pairs of segment with similar directions and within a fixed maximum distance from one to the other are reduced to the longest one.
2) Collinear segments with close endpoints are connected.
3) A second proximity check is applied to noncollinear segments to close small gaps in the network.
4) Finally, long chains of segments are simplified to the best approximating set, following [28].

The final result of this procedure is provided in Fig. 7(e) and shows that it is indeed possible to regularize the network by exploiting only very basic steps. The analysis is very fast and runs smoothly using generally valid parameters, which have been defined in [5] and shall not be changed into this approach.

IV. Experimental Results

The entire chain process has been tested on SAR imagery of urban areas recorded by the AIRSAR and AeS II airborne sensors. The sample used as an example throughout the discussion of the previous sections comes from the first data set. This AIRSAR scene was taken in 1994 in full-polarization mode with a ground spatial sampling of 5 m. The full image covers the area from the Pacific Ocean to inner Los Angeles near Hollywood, CA. The AeS II data set, on the other hand, has a ground spatial sampling of 0.5 m and depicts an area close to Munich, Germany. Ground truth data were obtained by manual photo interpretation of the AIRSAR image and by using a geographic information system layer for roads in the Munich area provided by the Landesamt fur Vermessung und Geoinformation of the Bavaria region. Both ground truth sets are in vector format and were compared with the vector list of road segments in the optimized final road network obtained at the end of the proposed processing chain (or at intermediate steps for comparison purposes).

In the following, three examples are provided, each aimed at showing one particular aspect of the proposed procedure and its advantages with respect to state of the art. Fig. 8 shows a second sample from the AIRSAR data set. By means of this example, it is possible to compare the effect of the junction-aware optimization with respect to the original version. Because the road grid here is very regular and the road extraction works

TABLE II
QUANTITATIVE EVALUATION AND COMPARISON OF THE RESULTS

	fig. 8(b)	fig. 8(c)
completeness	88.3%	90.8%
correctness	93.4%	91.4%
quality	83.1%	83.7%
	fig. 9(c)	fig. 7(e)
completeness	77.2%	87.9%
correctness	87.9%	85.7%
quality	69.7%	76.7%
		fig. 10(b)
completeness		76.9%
correctness		63.5%
quality		59.7%

(a) (b) (c)

Fig. 9. (a) Segments extracted from Fig. 2 using the algorithm introduced in [20]. (b) Segments extracted from Fig. 2 using the algorithm proposed in this paper. (c) Road network after junction-aware MRF optimization of the segments in (a).

well, it is expected that the MRF optimization with junction knowledge may be able to slightly improve the result. In fact, there is no major improvement between the original optimization [Fig. 8(b)] and the new result [Fig. 8(c)]. Only a few segments are added, and they do not introduce many junctions or lacking parts of the network. In some cases, false positives are added, but the overall visual impression is a strong similarity between the results.

For a more objective characterization, a numerical evaluation of the completeness, correctness, and quality indexes of the road network [29] were computed with respect to the ground truth in Fig. 8(d), and values are shown in Table II. As expected, completeness increases due to the added junctions, whereas correctness decreases because of more false positives. The two effects, however, do not compensate, and the overall quality slightly increases.

The second example, which is reported in Fig. 9, is aimed instead at highlighting the importance of the new road detector. This is done by proposing a visual comparison between the segments extracted from Fig. 4(c) by using the segment extraction procedure in [20] or the one introduced in this paper. It is interesting to note that the new algorithm allows a more precise extraction of long segments. MRF optimization, even considering junctions, is only partially able to recover problems introduced in Fig. 9(a), i.e., the artificially induced segmentation of long roads. Thus, the final road network in Fig. 9(c) is far less precise than the one in Fig. 7(e). Correspondingly, completeness and quality values, which are provided again in Table II, decrease as much as 10% and 7%, respectively.

(a) (b) (c)

Fig. 10. (a) Original image. (b) Road network after junction-aware MRF optimization of these segments. (c) Raster representation of the corresponding ground truth.

The final example in this section refers to Fig. 10, where the original AeS II image is close to the extracted final road network [Fig. 10(b)] and the corresponding ground truth [Fig. 10(c)]. Because this image was used as test data for [20], we use this example to compare the results of the procedure proposed in this paper with those in [20][Fig. 6(c)]. First, it is clear that the choice of approximating curvilinear lines with sequences of linear elements does not lead to sufficient accuracy in some areas of the image. However, regular patterns are visible. Even the highway roundabout, though poorly approximated, is more clearly visible in Fig. 10(b) than in our previous work. Correspondingly, index values in Table II increase by 15%–20% over those reported in [20]. Finally, the urban areas on the top right corner are now partially delineated, which is the most important result from the point of view of this paper, whereas in previous works, they were really hard to catch.

V. CONCLUSION

This paper shows that a careful exploitation of junction information may improve the road network extraction process in urban areas starting from high-resolution SAR images. This was done in two steps, namely: 1) designing a procedure for road candidate extraction that searches and identifies junctions, following the path of long roads even after these junctions and thus reducing unwanted segmentation of these roads, and 2) using candidate L- and T-shaped junctions, which improves the final result of the MRF optimization of the road network starting from the detected candidate roads.

Experimental results on two data sets in Section IV show that these two steps allow to achieve better quality values for the final extracted road network.

However, the same results also prove in two different situations that the process of urban area network extraction from high-resolution SAR images relies heavily on road candidate detection, i.e., the first part of this work. The less candidate segments fragmented, the better the result of the second part of this work, i.e., the optimization. Thus, future work will be devoted not only to refinement with more *a priori* information of the MRF model but also to improving the road detector proposed in this paper and making it more automatic and adaptive.

REFERENCES

[1] I. Couloigner, T. Ranchin, V. P. Valtonen, and L. Wald, "Benefit of the future SPOT-5 and of data fusion to urban roads mapping," *Int. J. Remote Sens.*, vol. 19, no. 8, pp. 1519–1532, 1998.

[2] F. Tupin, I. Bloch, and H. Maitre, "A first step toward automatic interpretation of SAR images using evidential fusion of several structure detectors," *IEEE Trans. Geosci. Remote Sensing*, vol. 37, no. 3, pp. 1327–1343, May 1999.

[3] B. Wessel, C. Wiedemann, and O. Hellwich, "Road extraction from multi-frequency and polarimetric SAR imagery," in *Proc. 4th Eur. Conf. Synthetic Aperture Radar*, Koln, Germany, Jun. 4–6, 2002, pp. 287–290.

[4] C. Weirong, W. Chao, and Z. Hong, "Road network extraction in high-resolution SAR images," in *Proc. IGARSS*, Anchorage, AK, Sep. 2004, vol. 6, pp. 3806–3809.

[5] F. Dell'Acqua, P. Gamba, and G. Lisini, "Road extraction aided by adaptive directional filtering and template matching," in *Proc. URBAN*, Tempe, AZ, Mar. 14–16, 2005, vol. 34, pt. 8/W27. Unformatted CD-ROM.

[6] H. Skriver, J. Schou, A. A. Nielsen, and K. Conradsen, "Polarimetric edge detector based on the complex Wishart distribution," in *Proc. IGARSS*, Sydney, Australia, Jul. 9–13, 2001, vol. 7, pp. 3149–3151.

[7] O. Hellwich and C. Streck, "Linear structures in SAR coherence data," in *Proc. IGARSS*, May 27–31, 1996, vol. 1, pp. 330–332.

[8] F. Tupin, H. Maitre, J.-F. Mangin, J.-M. Nicolas, and E. Pechersky, "Detection of linear features in SAR images: Application to road network extraction," *IEEE Trans. Geosci. Remote Sens.*, vol. 36, no. 2, pp. 434–453, Mar. 1998.

[9] C. Lacoste, X. Descombes, and J. Zerubia, "Road network extraction in remote sensing by Markov object process," in *Proc. ICIP*, Sep. 14–17, 2003, vol. 3, pp. 1017–1018.

[10] B.-K. Jeon, J.-H. Jang, and K.-S. Hong, "Road detection in spaceborne SAR images using a genetic algorithm," *IEEE Trans. Geosci. Remote Sens.*, vol. 40, no. 1, pp. 22–29, Jan. 2002.

[11] C. Steger, H. Mayer, and B. Radig, "The role of grouping for road extraction," in *Automatic Extraction of Man-Made Objects from Aerial and Space Images (II)*, A. Gruen, E. Baltsavias, and O. Henricsson, Eds. Cambridge, MA: Birkhaeuser, 1997, pp. 245–256.

[12] K. Price, "Urban street grid description and verification," in *Proc. IEEE Workshop Appl. Comput. Vis.*, pp. 148–154.

[13] S. Hinz and A. Baumgartner, "Automatic extraction of urban road networks from multi-view aerial imagery," *ISPRS J. Photogramm. Remote Sens.*, vol. 58, no. 1/2, pp. 83–98, 2003.

[14] U. Soergel, U. Thoennessen, and U. Stilla, "Visibility analysis of man-made objects in SAR images," in *Proc. 2nd GRSS/ISPRS Joint Workshop Remote Sens. and Data Fusion Over Urban Areas*, Berlin, Germany, May 22–23, 2003, pp. 120–124.

[15] G. Lisini, C. Tison, F. Tupin, and P. Gamba, "Feature fusion to improve road network extraction in high-resolution SAR images," *IEEE Geosci. Remote Sens. Lett.*, vol. 3, no. 2, pp. 217–221, Apr. 2006.

[16] F. Tupin, B. Houshmand, and M. Datcu, "Road detection in dense urban areas using SAR imagery and the usefulness of multiple views," *IEEE Trans. Geosci. Remote Sens.*, vol. 40, no. 11, pp. 2405–2414, Nov. 2002.

[17] R. Ruskone, S. Airault, and O. Jamet, "Road network interpretation: A topological hypothesis driven system," *Int. Arch. Photogramm. Remote Sens.*, vol. 30, no. 3/2, pp. 711–717, 1994.

[18] A. Barsi and C. Heipke, "Detecting road junctions by artificial neural networks," in *Proc. 2nd GRSS/ISPRS Joint Workshop Remote Sens. and Data Fusion Over Urban Areas*, Berlin, Germany, May 22–23, 2003, pp. 129–132.

[19] C. Wiedemann, "Improvement of road crossing extraction and external evaluation of the extraction results," *Int. Arch. Photogramm. Remote Sens.*, vol. 34, pt. 3-B, pp. 297–300, 2002.

[20] F. Dell'Acqua, P. Gamba, and G. Lisini, "Road map extraction by multiple detectors in fine spatial resolution SAR data," *Can. J. Remote Sens.*, vol. 29, no. 4, pp. 481–490, Aug. 2003.

[21] J. Chanussot, G. Mauris, and P. Lambert, "Fuzzy fusion techniques for linear features detection in multitemporal SAR images," *IEEE Trans. Geosci. Remote Sens.*, vol. 37, no. 3, pp. 1292–1305, May 1999.

[22] R. Huber and K. Lang, "Road extraction from high resolution Airborne SAR using operator fusion," in *Proc. IGARSS*, Sydney, Australia, Jul. 9–13, 2001, vol. 5, pp. 2813–2815.

[23] V. Karathanassi, C. Iossifidis, and D. Rokos, "A thinning-based method for recognizing and extracting peri-urban road networks from SPOT panchromatic images," *Int. J. Remote Sens.*, vol. 20, no. 1, pp. 153–168, Jan. 1999.

[24] F. Dell'Acqua and P. Gamba, "Detection of urban structures in SAR images by robust fuzzy clustering algorithms: The example of street tracking," *IEEE Trans. Geosci. Remote Sens.*, vol. 39, no. 10, pp. 2287–2297, Oct. 2001.

[25] J. Besag, "On the statistical analysis of dirty pictures," *J. R. Statist. Soc., B*, vol. 48, no. 3, pp. 259–302, 1986.

[26] P. Gamba, F. Dell'Acqua, and G. Lisini, "Improving urban road extraction in high-resolution images exploiting directional filtering, perceptual grouping, and simple topological concepts," *IEEE Geosci. Remote Sens. Lett.*, vol. 3, no. 3, pp. 387–391, Jul. 2006.

[27] S. Vasudevan, R. Cannon, and J. Bezdek, "Heuristics for intermediate level road finding algorithms," *Comput. Vis., Graph., Image Process.*, vol. 44, no. 2, pp. 175–190, Nov. 1988.

[28] D. Douglas and T. Peucker, "Algorithms for the reduction of the number of points required to represent a digitized line or its caricature," *Can. Cartogr.*, vol. 10, no. 2, pp. 112–122, 1973.

[29] C. Wiedemann, "External evaluation of road networks," *Int. Arch. Photogramm. Remote Sens. Spatial Inf. Sci.*, vol. 34, pt. 3W/8, pp. 93–98, 2003.

Matteo Negri was born in Lecco, Italy, in 1978. He received the laurea degree in electronic engineering from the University of Pavia, Pavia, Italy, in 2005. His thesis involved the development of a processing framework for road network extraction from high-resolution synthetic aperture radar images.

He is currently with Digitec Lecco srl, Montecchio Maggiore, Italy, where he works on license plate recognition systems. His main interests are dynamic and synoptic meteorology, digital vision, programming languages, web publishing, and graphic design.

Paolo Gamba (S'91–M'93–SM'00) received the laurea (cum laude) and Ph.D. degrees from the University of Pavia, Pavia, Italy, in 1989 and 1993, respectively, both in electronic engineering.

He is currently an Associate Professor of telecommunications with the University of Pavia. He has published more than 40 papers in peer-review journals on urban remote sensing and presented more than 100 papers at workshops and conferences. He gave a tutorial on "Urban Remote Sensing Applications" at IGARSS'04 and was invited to present his work about urban remote sensing by SAR satellites at the Jet Propulsion Laboratory, the University of Utah, and the Technical University of Berlin. His current research interests include remote sensing data fusion for urban applications, especially SAR urban analysis, multitemporal/polarization/frequency and multispectral data classification by neural and fuzzy classification tools, satellite image interpretation for civil protection purposes, and weather radar and meteorological satellite data interpretation.

Dr. Gamba is the Organizer and Technical Chair of the biennial GRSS/ISPRS Joint Workshops on "Remote Sensing and Data Fusion over Urban Areas" from 2001 to 2007. From October 2002 to October 2004, he was Chair of Technical Committee 7 "Pattern Recognition in Remote Sensing" of the International Association for Pattern Recognition (IAPR), whose purpose is to foster research in image processing and pattern recognition techniques applied to photogrammetric and remote sensing issues. He is an Associate Editor of the IEEE GEOSCIENCE AND REMOTE SENSING LETTERS and currently the Chair of the Data Fusion Committee of the IEEE Geoscience and Remote Sensing Society. He is or has been the Guest Editor of a special issue of the ISPRS *Journal of Photogrammetry and Remote Sensing* on "Algorithm and Techniques for Multi-Source Data Fusion in Urban Areas," two Special Sections of the IEEE TRANSACTIONS ON GEOSCIENCE AND REMOTE SENSING on "Urban Remote Sensing" and "Disaster Assessment and Management by Remote Sensing," a Special Issue of the *International Journal of Information Fusion* on "*Fusion of Urban Remotely Sensed Features*," and a special issue of *Pattern Recognition Letters* on "Pattern Recognition in Remote Sensing."

Gianni Lisini (S'00–M'04) was born in Voghera, Italy, on April 25, 1977. He received the laurea and Ph.D. degrees, in 2002 and 2005, respectively, from the University of Pavia, Pavia, Italy, both in electronics engineering.

His previous research interest is the analysis of remotely sensed data, mainly in the field of pattern recognition in urban and suburban areas. His current research interests include several typologies of images and resolutions, multiband classification of low-resolution synthetic aperture radar images, and hyperspectral and multispectral very high resolution images. He passed the qualification exam for practicing the profession of engineering in November 2002.

Florence Tupin (M'06) received the engineering and Ph.D. degrees from the École Nationale Supérieure des Télécommunications (ENST), Paris, France, in 1994 and 1997, respectively.

She is currently an Associate Professor with the Traitement du Signal et des Images, ENST. Her research interests are image analysis and interpretation, three-dimensional reconstruction, Markov random field techniques, and synthetic aperture radar remote sensing.